Monte Carlo simulations of polyampholyte-polyelectrolyte complexes: Effect of charge sequence and strength of electrostatic interactions

Junhwan Jeon and Andrey V. Dobrynin*
Polymer Program, Institute of Materials Science and Department of Physics, University of Connecticut, Storrs, Connecticut 06269-3136, USA
(Received 3 February 2003; published 26 June 2003)

We present the results of Monte Carlo simulations of complexation between polyampholyte and polyelectrolyte chains. Polymers are modeled as bead-spring chains of charged Lennard-Jones particles each consisting of 32 monomers. Formation of a polyampholyte-polyelectrolyte complex is driven by polarization-induced attractive interactions. The complex is usually formed at the end of the polyelectrolyte with the polyampholyte chain elongated and aligned along the polyelectrolyte backbone. This complex structure between the polarized polyampholyte chain and the polyelectrolyte leads to maximization of the attractive and minimization of the repulsive electrostatic interactions. The size of a polyampholyte in a complex is usually larger than that of an isolated polyampholyte chain. We also observed that initially collapsed polyampholytes undergo a coil-globule transition by forming a complex. The structure of a polyampholyte-polyelectrolyte complex was analyzed by tail and loop distribution functions. We have found that the number of loops increases while their sizes decrease with the strength of the electrostatic interactions. Polyampholytes with random charge sequence form stronger complexes with polyelectrolytes than those with alternating charge sequence. Polyampholytes with long blocky sequences form a double helix with a polyelectrolyte at sufficiently large values of the Bjerrum length.

DOI: 10.1103/PhysRevE.67.061803 PACS number(s): 36.20.−r, 61.20.Qg, 87.15.−v

I. INTRODUCTION

Considerable theoretical and experimental work during the last half a century has been devoted to charged polymers [1–9]—macromolecules with ionizable groups. Under appropriate conditions, such as in aqueous solutions, these groups dissociate, leaving ions on chains and counterions in solution. If the charges on polymers are all positive or all negative, these polymers are called polyelectrolytes. Common polyelectrolytes are polyacrylic and methacrylic acids and their salts, sulfonated polystyrene, cellulose derivatives, DNA, and other polyacids and polybases. If, after dissociation of the charged groups, the polymers carry both positive and negative charges, they are called polyampholytes. Examples of polyampholytes include proteins, for example gelatin, bovine serum albumin (BSA), and synthetic copolymers made of monomers with acidic and basic groups. If these groups are weak acids or bases, the net charge on the polyampholyte can be changed by varying the pH of aqueous solutions and at high charge asymmetry these polymers demonstrate polyelectrolytelike behavior.

Soluble complexes between polyampholytes and polyelectrolytes are well-documented in the literature [9–18]. When the polyampholyte has a weak net negative charge it binds to anionic polyelectrolytes to form a complex that remains in an aqueous solution. Fibrillar proteins such as actin, collagen, and fibrinogen are sufficiently rigid that they have an open structure, allowing easy access to the amino acids of opposite charge to the polyelectrolyte. For example, fibrinogen is known to bind to sulfonated polystyrene [19]. Denatured proteins such as gelatin (denatured collagen) are flexible random coils in water. Such coils polarize in the presence of the polyelectrolyte, putting their oppositely charged amino acids close to the polyelectrolyte. Insoluble complexes [6] are formed when the net charge on the polyampholyte is of opposite sign to the charge on the polyelectrolyte. Complexation between polyampholyte and polyelectrolyte chains is controlled by ionic strength, pH, concentration of polymeric components, and molecular weight of polymers [15].

Globular proteins such as albumin and γ-globulins are also known to form soluble complexes with flexible polyelectrolytes of the same net charge. For globular proteins it is not yet clear whether the proteins denature on binding, assume a different form, or maintain their native form with the polyelectrolyte adapting its conformation to facilitate binding. An important example of complexes with globular proteins is found in synovial fluid, where the anionic polyelectrolyte sodium hyaluronate binds with a variety of proteins [20–23].

Recent theoretical studies [24–29] of polyampholyte adsorption on charged objects supported the idea that polarization of polyampholytes in the external electric field created by a charged object is the major factor leading to their strong interaction with these objects. For example, polarization-induced attraction between polyampholytes and charged surface can lead to multiple adsorbed polymeric layers. The structure and thickness of these layers depends on the charge distribution along the polyampholyte backbone, which determines the polarizability of polyampholyte chains in external electric fields [30–34], solution concentration, surface curvature, and surface charge density. This theory of polyampholyte adsorption on charged surfaces is in good qualitative agreement with experimental results [35–43].

*Electronic address: avd@ims.uconn.edu

The aim of the present paper is to test the idea of polarization-induced attractive interactions between polyampholyte and polyelectrolyte chains and to show how their complexation can be influenced by the charge sequence along the polyampholyte backbone and the strength of the electrostatic interactions. To answer these questions, we performed Monte Carlo simulations of polyampholyte-polyelectrolyte complexes formed by a fully charged polyelectrolyte chain and a symmetric polyampholyte molecule carrying an equal number of positive and negative charges. The rest of the paper is organized as follows. The simulation model and the algorithm are described in Sec. II. Section III gives a detailed account of the simulation results for the complexation threshold dependence on the charged sequence, distribution of the charged monomers within a complex, as well as the dependence of the complex size, the tail and loop distribution funcitons on the strength of the electrostatic interactions. Finally, in conclusion (Sec. IV) we discuss our results.

II. MODEL AND METHODS

In our simulations all polymers are modeled as bead-spring chains of charged Lennard-Jones particles. Polyelectrolyte has $N_{PE}=32$ negatively charged beads while polyampholyte contains $N_{PA}=32$ repeat units with an equal number of positive and of negative charges. All beads interact via the truncated-shifted Lennard-Jones (LJ) potential,

$$U_{LJ}(r)=\begin{cases} 4\varepsilon_{LJ}\left[\left(\frac{\sigma}{r}\right)^{12}-\left(\frac{\sigma}{r}\right)^{6}-\left(\frac{\sigma}{r_c}\right)^{12}+\left(\frac{\sigma}{r_c}\right)^{6}\right], & r\leqslant r_c \\ 0, & r>r_c, \end{cases} \tag{1}$$

where r is the distance between two beads, σ is the bead diameter, and the cutoff distance r_c is equal to 2.5σ. The parameter ε_{LJ} determines the strength of the short-range interactions and is set to $\varepsilon_{LJ}=0.35k_BT$, where k_B is the Boltzmann constant and T is the absolute temperature. This choice of the parameter $\varepsilon_{LJ}=0.35k_BT$ corresponds to a theta condition [44] for a neutral polymer chain.

The connectivity of beads into a chain is maintained by the finite extension nonlinear elastic (FENE) potential,

$$U_{FENE}(r)=-\frac{1}{2}kR_0^2\ln\left(1-\frac{r^2}{R_0^2}\right), \tag{2}$$

where $k=7k_BT/\sigma^2$ is the spring constant and $R_0=2\sigma$ is the maximum bond length at which the elastic energy of the bond becomes infinite. The FENE potential only gives the attractive part of the bond potential. The repulsive part of the bond potential is provided by the shifted LJ potential [see Eq. (1) above].

The solvent is modeled by a dielectric medium with the dielectric constant ε. In such a continuous representation of the solvent, all charged particles separated by distance r_{ij} interact with each other via the unscreened Coulomb potential

$$U_{Coul}(r_{ij})=k_BT\frac{l_Bq_iq_j}{r_{ij}}, \tag{3}$$

where q_i is the valence of a charged bead. The strength of the electrostatic interactions is controlled by the Bjerrum length $l_B=e^2/(\varepsilon k_BT)$, defined as the length scale at which the Coulomb interaction between two elementary charges e in a dielectric medium with dielectric constant ε is equal to the thermal energy k_BT. In water at room temperature the Bjerrum length is about 7 Å. We performed simulations of complex formations in a system of chains with the values of the Bjerrum length $l_B=2\sigma-6\sigma$. In our simulations we consider complex formation at infinite dilution and neglect the effect of counterions.

Two different types of moves are used in our simulations: (i) translational move of a single bead and (ii) pivot rotation move of chain section. A translational move is performed in such a way that a displacement $\Delta\vec{r}=(\Delta x,\Delta y,\Delta z)$ of a randomly selected bead is chosen randomly from the intervals $-0.5\sigma\leqslant\Delta x,\ \Delta y,\ \Delta z\leqslant 0.5\sigma$. For a pivot rotation move, two beads in a chain are initially selected at random thus dividing a chain into two or three sections. Then the randomly chosen chain section is rotated on a random angle around the axes drown through two selected beads. This pivot rotation move [45,46] is carried out after every Monte Carlo (MC) step (attempted trial move per bead) is completed. The acceptance of the pivot rotation moves in our simulation is about 40%.

At the beginning of each simulation run both chains were preequilibrated for 5×10^6 MC steps. For the considered range of parameters after a preequilibration run the polyampholyte is in a collapsed globule state while the polyelectrolyte is in an elongated rodlike conformation. At the beginning of the simulation run the polyampholyte is placed in the middle of the polyelectrolyte chain at a distance of the order of its radius of gyration from the polyelectrolyte backbone. Then the system is allowed to equilibrate for additional 1.6×10^6 MC steps. The production run lasts another 1.6×10^7 MC steps. For random polyampholytes various properties of polyampholyte-polyelectrolyte complexes obtained during the production run were also averaged over 70 different charge sequences.

III. RESULTS AND DISCUSSION

A. Position of polyampholytes in a complex

The evolution of the complex structure formed by random polyampholyte and polyelectrolyte chains during the simulation run is shown in Fig. 1. As mentioned earlier, a collapsed polyampholyte is initially placed in the middle of a polyelectrolyte chain. In earlier stages of the simulation run, the polyampholyte chain is polarized by the external electric field created by the polyelectrolyte chain by stretching out perpendicular to the polyelectrolyte backbone in such a way that oppositely charged monomers are located closer to the polyelectrolyte while similarly charged ones are farther away from it. During the simulation run, the polyampholyte migrates towards the end of the polyelectrolyte chain, maintain-

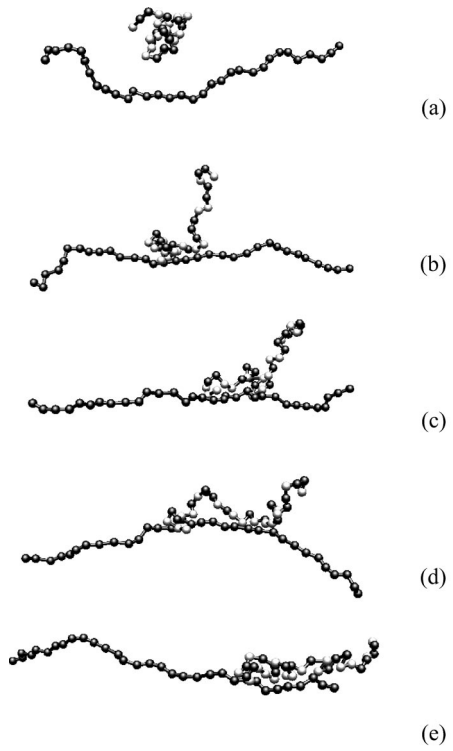

FIG. 1. Evolution of structure of random polyampholyte-polyelectrolyte complex with the value of the Bjerrum length $l_B = 5\sigma$ during the simulation run at (a) 0 Monte Carlo steps (MCS), (b) 10 000 MCS, (c) 50 000 MCS, (d) 100 000 MCS, and (e) 500 000 MCS. Dark spheres correspond to negatively charged beads and white ones to positively charged beads.

ing its elongated shape. The elongated part of the polyampholyte forms an angle with the polyelectrolyte backbone. The migration of the polyampholyte towards the end of the polyelectrolyte proceeds by forming a long loop or by moving back and forth while positively charged beads are in contact with the polyelectrolyte. Once the polyampholyte reaches the end of the polyelectrolyte, it usually keeps its position and rarely moves to another end of the polyelectrolyte. This tells us that the energy barrier for the polyampholyte to move back to the middle of the polyelectrolyte chain is higher than the thermal energy k_BT.

Figure 2 shows snapshots of complexes formed by randomly and alternatively charged polyampholytes and polyelectrolytes at different values of the Bjerrum length. The polyelectrolyte in each complex has a rodlike shape regardless of the strength of the electrostatic interaction and the charge sequence on the polyampholyte chain. Polyampholytes that were initially in a collapsed globule state adopt an elongated conformation oriented along the polyelectrolyte backbone.

To quantify the results shown in Fig. 2, during the production runs we have calculated the distribution function $P(R_{PA})$ of the center of mass of the polyampholyte chain in a complex (see Fig. 3). The position of the center of mass of the polyampholyte chain R_{PA} is measured with respect to the center of mass of the polyelectrolyte chain. For random polyampholytes this distribution function was also averaged over 70 different charge realizations. As indicated by the position of the maximum in the distribution function (see Fig. 3), both types of polyampholytes with random and alternating charge sequences form a complex at the end of

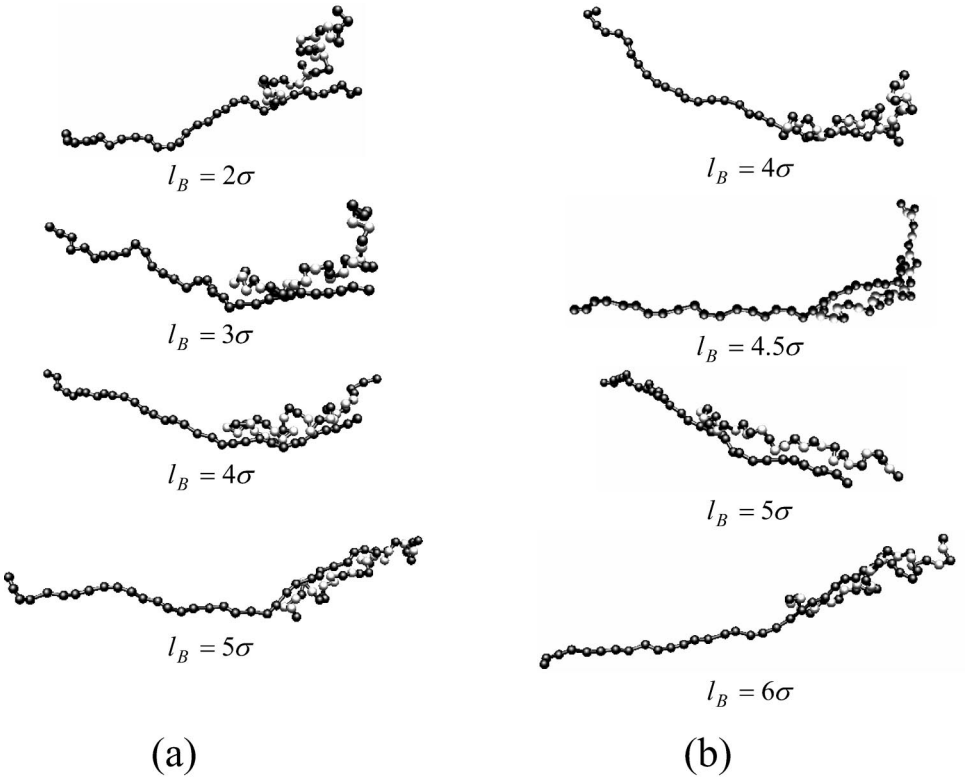

FIG. 2. Typical conformations of polyampholyte-polyelectrolyte complexes at different values of the Bjerrum length l_B. (a) Random polyampholyte-polyelectrolyte complexes and (b) alternating polyampholyte-polyelectrolyte complexes. Dark spheres correspond to negatively charged beads and white ones to positively charged beads.

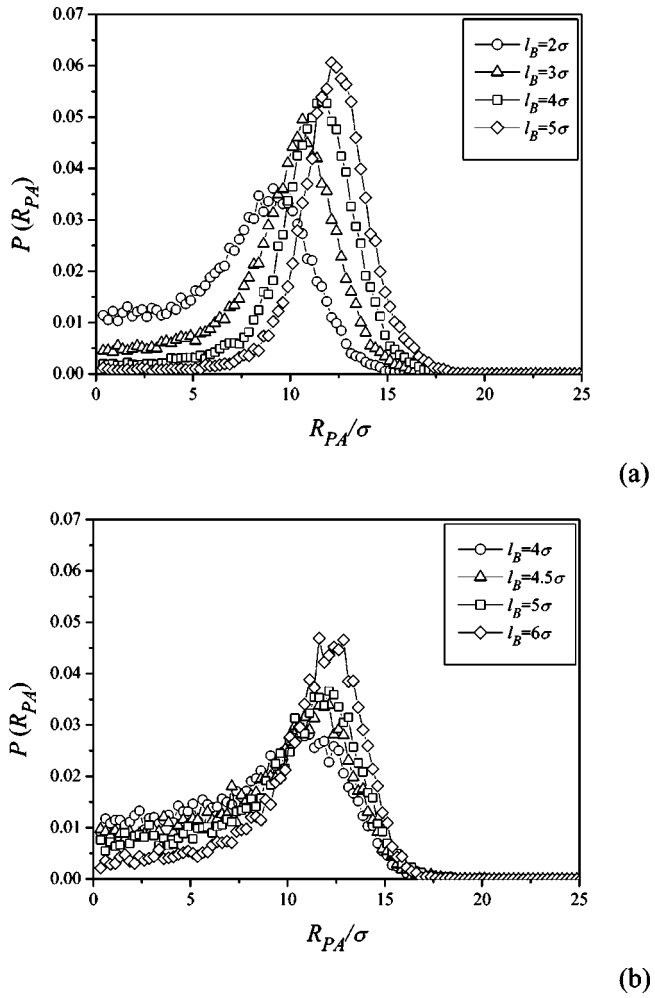

FIG. 3. Dependence of the distribution function $P(R_{PA})$ of the position of center of mass R_{PA} of (a) random polyampholyte and (b) alternating polyampholyte on the value of the Bjerrum length l_B.

polyelectrolyte chain. For random polyampholytes, the maximum in the distribution function moves closer to the end of the polyelectrolyte and the distribution function narrows as the value of the Bjerrum length l_B increases. The maximum is located at $R_{PA}=9.1\sigma$ for the value of the Bjerrum length $l_B=2\sigma$. It shifts to $R_{PA}=12.1\sigma$ at $l_B=5\sigma$ while increasing its height at the same time. The standard deviation of the distribution function is 3.72σ and 2.26σ at the value of the Bjerrum length $l_B=2\sigma$ and 5σ, respectively. In the case of alternating polyampholytes, the distribution function of the center of mass does not show such a drastic change with an increase in the strength of the electrostatic interactions. The maximum of the distribution function shifts only by 0.5σ from 11.1σ at $l_B=4\sigma$ to 11.6σ at $l_B=6\sigma$. The distribution function stays broad and asymmetric even when the Bjerrum length is equal to its largest value, $l_B=6\sigma$.

B. Polarization of polyampholytes in a complex

The quantitative information about the change in each chain's conformation as they form a complex can be obtained by analyzing the mean-square radius of gyration $\langle R_g^2\rangle$,

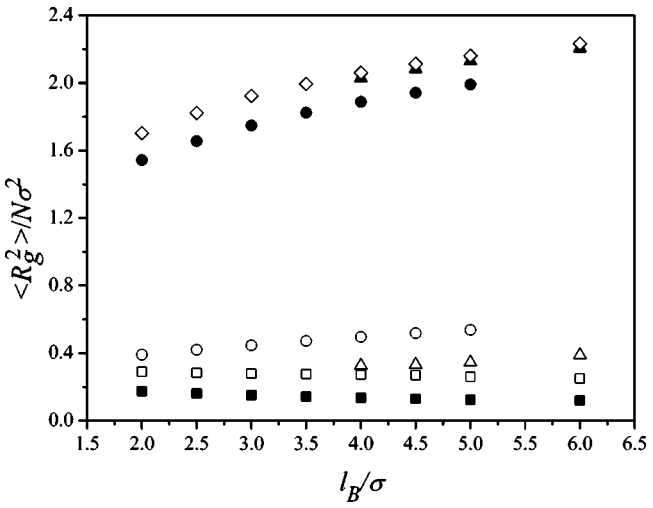

FIG. 4. Dependence of the normalized value of the mean-square radius of gyration $\langle R_g^2\rangle$ on the value of the Bjerrum length of polyelectrolyte in random polyampholyte-polyelectrolyte complex (●), polyampholyte in random polyampholyte-polyelectrolyte complex (○), polyelectrolyte in alternating polyampholyte-polyelectrolyte complex (▲), polyampholyte in alternating polyampholyte-polyelectrolyte complex (△), isolated random polyampholyte (■), isolated alternating polyampholyte (□), and isolated polyelectrolyte (◇).

$$\langle R_g^2\rangle=\left\langle \frac{1}{N}\sum_{i=1}^{N}(\vec{r}_i-\vec{r}_{\text{c.m.}})^2\right\rangle, \tag{4}$$

and the mean-square end-to-end distance $\langle R_e^2\rangle$,

$$\langle R_e^2\rangle=\langle(\vec{r}_N-\vec{r}_1)^2\rangle. \tag{5}$$

In Eqs. (4) and (5) $\vec{r}_i$ is the position vector of the ith bead and $\vec{r}_{\text{c.m.}}$ is the position vector of the chain center of mass. The summation in Eq. (4) is carried out over all beads on a chain.

Figure 4 shows the variations of the swelling parameter for chains in a complex as a function of the Bjerrum length. For comparison, the variation of the chain size of isolated chains is also shown in this figure. The size of polyampholytes in a complex is usually larger than that of isolated polyampholyte chains. Furthermore, random polyampholytes in a complex have a larger size than alternating ones. It also can be seen that the size of isolated polyampholytes decreases as the value of the Bjerrum length increases. However, the size of the polyampholyte chain in a complex shows an opposite trend. Such an increase in the size of the polyampholyte chains is due to their polarization in the external electric field created by a polyelectrolyte. The attraction between the polyelectrolyte and oppositely charged beads on the polyampholyte chain leads to weak contraction of the polyelectrolyte chain in a complex. As a result, the size of the polyelectrolyte in a complex is smaller than that of an isolated polyelectrolyte chain.

To examine the shape variations of polyampholyte and polyelectrolyte chains in a complex, we use the shape ratio

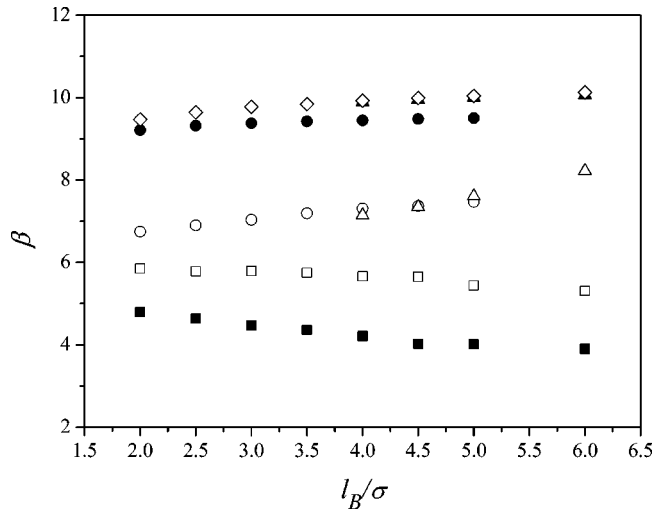

FIG. 5. Dependence of the shape ratio $\beta=\langle R_e^2\rangle/\langle R_g^2\rangle$ on the Bjerrum length l_B. Notations are the same as in Fig. 4.

$$\beta=\langle R_e^2\rangle/\langle R_g^2\rangle. \tag{6}$$

The shape ratio β is equal to 6 for a random coil and is equal to 12 for a rigid rod. Figure 5 shows variation of the shape ratio β for chains in a complex. The shape ratio of polyelectrolyte chains in a complex stays almost unchanged through the entire range of the Bjerrum lengths. It is also slightly smaller than that of an isolated polyelectrolyte chain, again indicating contraction of a polyelectrolyte in a complex. However, the shape ratio β for polyampholytes in a complex increases with increasing the strength of electrostatic interactions. For random polyampholytes, the shape ratio β is equal to 6.7 at $l_B=2\sigma$ and increases to 7.4 for the value of the Bjerrum length $l_B=5\sigma$. Such a change in the shape ratio means that polyampholyte chains become more elongated as the strength of electrostatic interactions increases. However, the shape ratio β for alternating polyampholytes increases

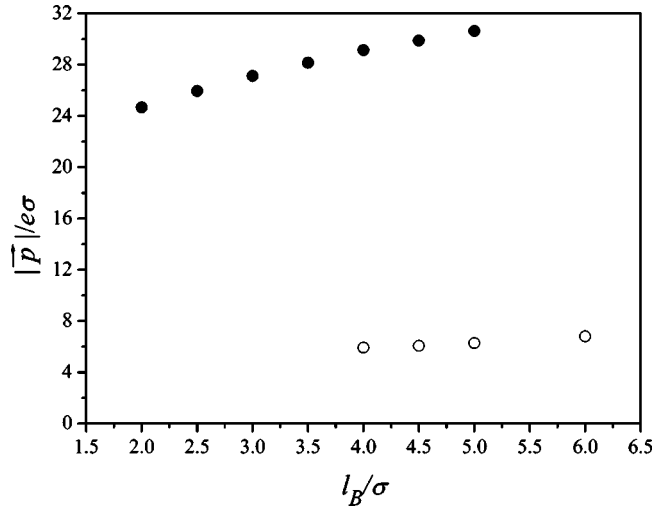

FIG. 6. Dependence of the absolute value of the dipole moment on the Bjerrum length l_B for random (●) and for alternating (○) polyampholytes.

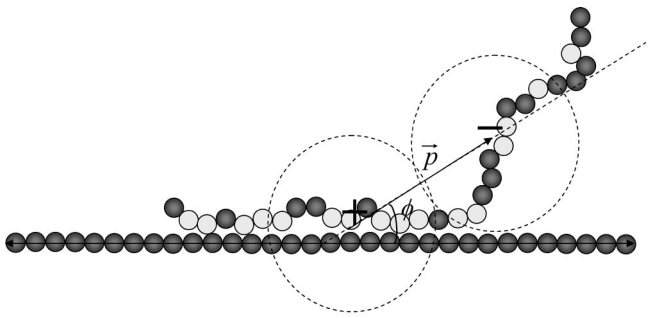

FIG. 7. Schematic sketch of random polyampholyte-polyelectrolyte complex showing definitions of the dipole moment of polyampholyte and its orientation with respect to the end-to-end vector of the polyelectrolyte chain.

faster with the Bjerrum length than that for random ones. This is due to regular charge sequence—alternating polyampholytes in a complex are able to stretch out more efficiently with the polyelectrolyte chain forming zig-zag-like structure.

The electric dipole moment

$$\vec{p}=\sum_{i=1}^{N_{PA}} eq_i\vec{r}_i \tag{7}$$

provides further information about polarization of the polyampholyte chain in a complex. The absolute value of the electric dipole moment $|\vec{p}|$ shows how far the center of mass of positively charged beads is separated from that of the negatively charged ones. Obviously, the larger the value of the electric dipole moment $|\vec{p}|$, the more strongly the polyampholyte chain is polarized. Figure 6 shows the dependence of the value of the electric dipole moment $|\vec{p}|$ of a polyampholyte chain on the strength of the electrostatic interactions. The value of the dipole moment $|\vec{p}|$ for random polyampholytes is always larger than that of alternating ones

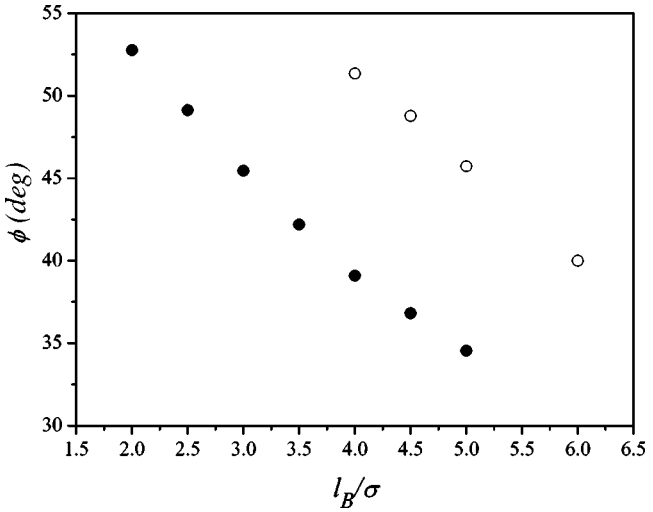

FIG. 8. Dependence of the angle ϕ between the direction of the dipole moment of polyampholyte chain and the end-to-end vector of polyelectrolyte chain on the Bjerrum length l_B for random (●) and alternating (○) polyampholytes.

at the same strength of the electrostatic interactions. In fact, the value of the electric dipole moment $|\vec{p}|$ for alternating polyampholytes stays almost unchanged for our considered range of the Bjerrum lengths. This means that alternating polyampholytes have limited polarizability.

Another important characteristic of the complex structure is the orientation of the dipole moment $\vec{p}$. Figure 7 shows our definition of the angle ϕ between the direction of the electric dipole moment $\vec{p}$ and polyelectrolyte backbone. The angle ϕ is always smaller than 55° (see Fig. 8). With increasing the strength of electrostatic interactions, the induced electric dipole moment of a polyampholyte aligns along the end-to-end vector of a polyelectrolyte chain leading to a decrease in the value of the angle Judging from Fig. 6, random polyampholytes have higher polarization ability than alternating ones, aligning better with a polyelectrolyte chain that results in smaller values of the angle ϕ.

C. Distribution of loops and tails in a complex

Detailed information about complex structure can be obtained by analyzing tail and loop distribution functions. A tail is defined as a sequence of bonds beginning from a chain end to the first bead in contact with a polyelectrolyte. Below we assume that two beads are in contact with each other if the distance between their centers of mass is smaller than or equal to their diameter σ. The number of bonds in a tail varies between 1 and $N_{PA}-1$. A loop is defined as a sequence of bonds between two nearest monomers along the chain backbone that are in contact with a polyelectrolyte. Thus, the minimum length of a loop is 1 and the maximum length of a loop is $N_{PA}-1$. Let us define the probability to find a tail $P_{tail}(i)$ and a loop $P_{loop}(i)$ with i bonds as follows:

$$P_{tail}(i)=\frac{N_{tail}(i)}{\sum_{i=1}^{N_{PA}-1} N_{tail}(i)} \tag{8}$$

and

$$P_{loop}(i)=\frac{N_{loop}(i)}{\sum_{i=1}^{N_{PA}-1} N_{loop}(i)}, \tag{9}$$

where $N_{tail}(i)$ and $N_{loop}(i)$ are the total numbers of tails and loops with the number of bonds i observed during the simu-

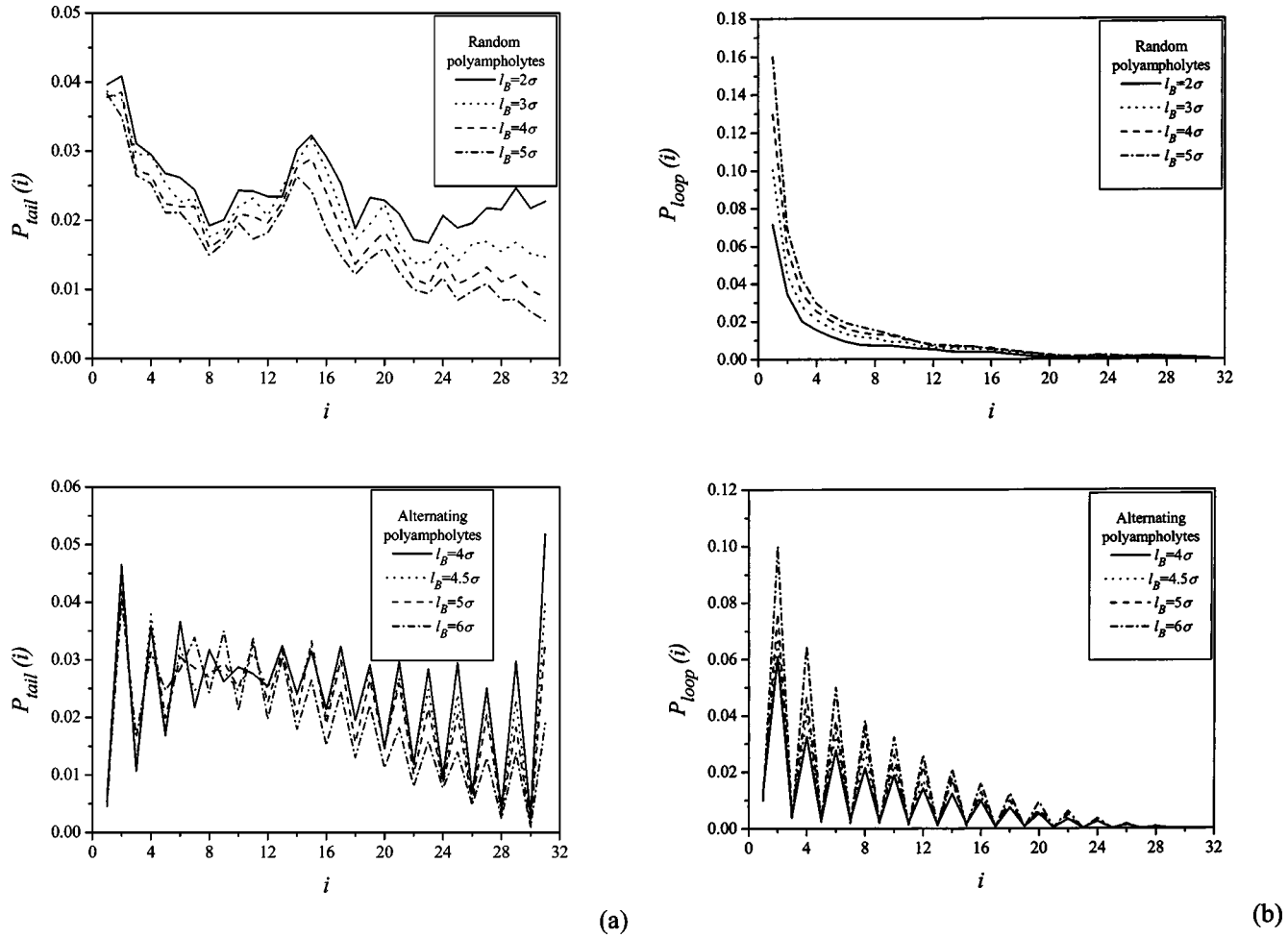

FIG. 9. (a) Tail $P_{tail}(i)$ and (b) loop $P_{loop}(i)$ distribution functions for random and alternating polyampholytes.

lation run. Figure 9 shows the dependence of the tail $P_{tail}(i)$ and loop $P_{loop}(i)$ distribution functions on the value of the Bjerrum length l_B. For random polyampholytes the bimodal form of the tail distribution function [see Fig. 9(a)] with higher probabilities of short $P_{tail}(1)$ and long $P_{tail}(15)$ tails agrees well with the structure of the complex shown in Fig. 2. According to this figure, half of the polyampholyte chain is aligned parallel to a polyelectrolyte forming a train of small loops while the other half forms a long tail. Generally, the probability to find a short loop $P_{loop}(1)$ is much higher than that for any other loop sizes $P_{loop}(i)$ [see Fig. 9(b)]. This tells us that the majority of contacts in complexes are formed by consecutive beads. In the case of alternating polyampholytes, tail and loop distribution functions are repeating the alternating charge sequence. When the Bjerrum length l_B is equal to 4σ, the probability of the longest tail $P_{tail}(31)$ is highest [see Fig. 9(a)]. Such a distribution function is possible if there is only one bead located at the end of the polyampholyte chain in contact with a polyelectrolyte. This propensity in the tail distribution function disappears with increasing strength of electrostatic interaction. The loop distribution function for an alternating polyampholyte clearly shows that most loops have an even number of bonds [see Fig. 9(b)]. Furthermore, the large value of $P_{loop}(2)$ indicates that almost all oppositely charged beads are in contact with the polyelectrolyte backbone.

Further analysis of the loop structure can be done by calculating the average loop size

$$\langle i\rangle_{loop}=\frac{\sum_{i=1}^{N_{PA}-1} iP_{loop}(i)}{\sum_{i=1}^{N_{PA}-1} P_{loop}(i)}. \tag{10}$$

With increasing strength of the electrostatic interactions, the average loop size decreases for both random and alternating polyampholytes (see Fig. 10). The decrease in the average loop size is consistent with the increase in the average number of contacts $\langle N_c\rangle$ between polyelectrolyte and polyampholyte chains in a complex as the value of the Bjerrum length increases. There is about one contact per chain at the Bjerrum length $l_B=2\sigma$ for random polyampholytes and at $l_B=4\sigma$ for alternating ones. Such a trend agrees with the fact that no complexes were formed below $l_B=2\sigma$ for random and below $l_B=4\sigma$ for alternating polyampholytes.

D. Effect of block charge sequence on complexation

So far we have compared complexes made of random and alternating polyampholytes. In this section we study the effect of block length of polyampholytes on the complex structure. In our simulations we studied block polyampholytes where the number of monomers in a block is $N_{block}=1$, 2, 4, 8, and 16. The distribution function $P(R_{PA})$ of the center of mass of a polyampholyte chain in a complex at the value of the Bjerrum length $l_B=4\sigma$ is shown in Fig. 11. This figure shows that the more charges a block has, the larger the amplitude is of the maximum of the distribution function. However, the position of the maximum does not change much until the block size reaches 4. For polyampholytes where the number of charges in each block is 8, the maximum of the distribution function shifts to the right, meaning that a whole polyampholyte is moving closer to the end of a polyelectrolyte chain. The distribution function becomes sharper and more symmetric as the block length increases.

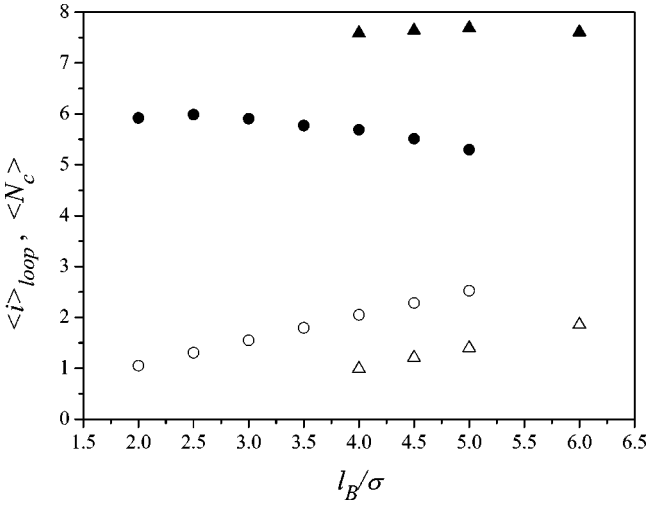

FIG. 10. Dependence of the average number of bonds $\langle i\rangle_{loop}$ in a loop (filled symbols) and the average number of contacts $\langle N_c\rangle$ between polyampholyte and polyelectrolyte (open symbols) on the Bjerrum length l_B for random (●,○) and alternating (▲,△) polyampholytes.

Polyampholytes with sufficiently long blocky charge sequences, such as $N_{block}=8$ and 16, and a Bjerrum length larger than 3σ, intertwine with a polyelectrolyte backbone-forming double helix. The double helix structure consists of monomers from one block of the polyampholyte, which are positioned at the end of a block polyampholyte, and the same number of monomers from the polyelectrolyte chain. Snapshots of the double helix structure are shown in Figs. 12(c)

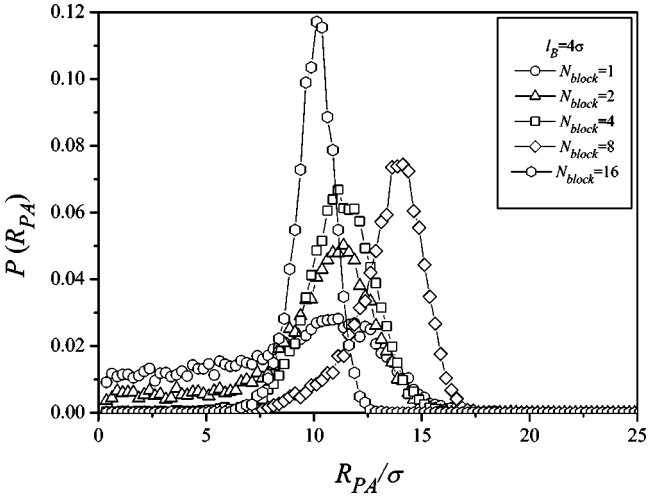

FIG. 11. Distribution function $P(R_{PA})$ of the position of center of mass R_{PA} of block polyampholytes at the value of the Bjerrum length $l_B=4\sigma$.

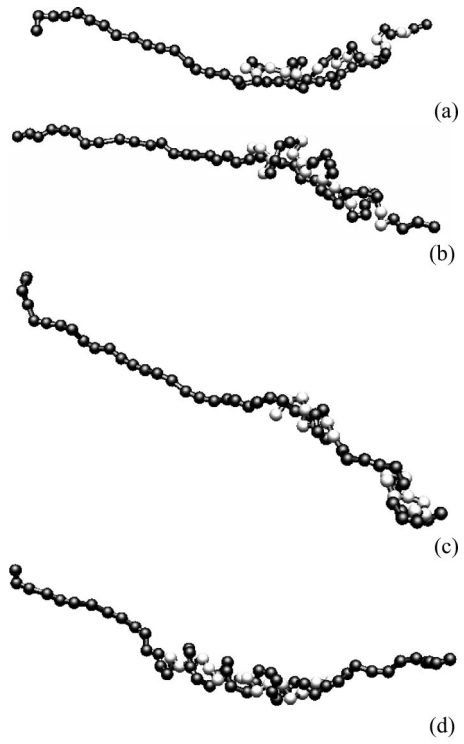

FIG. 12. Typical conformations of block polyampholyte-polyelectrolyte complexes with block length (a) $N_{block}=2$; (b) $N_{block}=4$; (c) $N_{block}=8$; (d) $N_{block}=16$ at the value of the Bjerrum length $l_B=4\sigma$. Dark spheres represent negatively charged beads and white ones positively charged beads.

and 12(d). The local structure of the double helix resembles a double helix formed by two oppositely charged polyelectrolyte chains. Recently, Winkler *et al.* [47] reported that oppositely charged polyelectrolytes form a collapsed conformation and a stretched double helix depending on the chain length and value of the Coulomb interaction parameter. When the Coulomb interaction parameter is large enough, collapsed structures were found for all chain lengths. In our simulation, we found that the double helix structures are stable for all values of the Bjerrum lengths. It is stabilized by the electrostatic repulsion between similarly charged blocks and the polyelectrolyte chain.

The shape ratio β for polyelectrolyte chains in a complex shows a weak dependence on the strength of the electrostatic interactions [see Fig. 13(a)]. However, the polyelectrolyte chains contract to a greater extent in complexes formed by polyampholytes with longer blocks. For example, the shape ratio β for a polyelectrolyte in a complex with a polyampholyte with $N_{block}=8$ is smaller than 9.0, showing significant contraction of the polyelectrolyte in the complex. Because of the formation of a double helix structure for polyampholytes with $N_{block}=16$, the polyelectrolyte chain undergoes a larger contraction than in any other case. The shape ratio β for block polyampholytes increases with the strength of the electrostatic interactions and with the block length [see Fig. 13(b)]. In the case of a polyampholyte built of blocks with $N_{block}=8$ and 16, the shape ratio β levels off

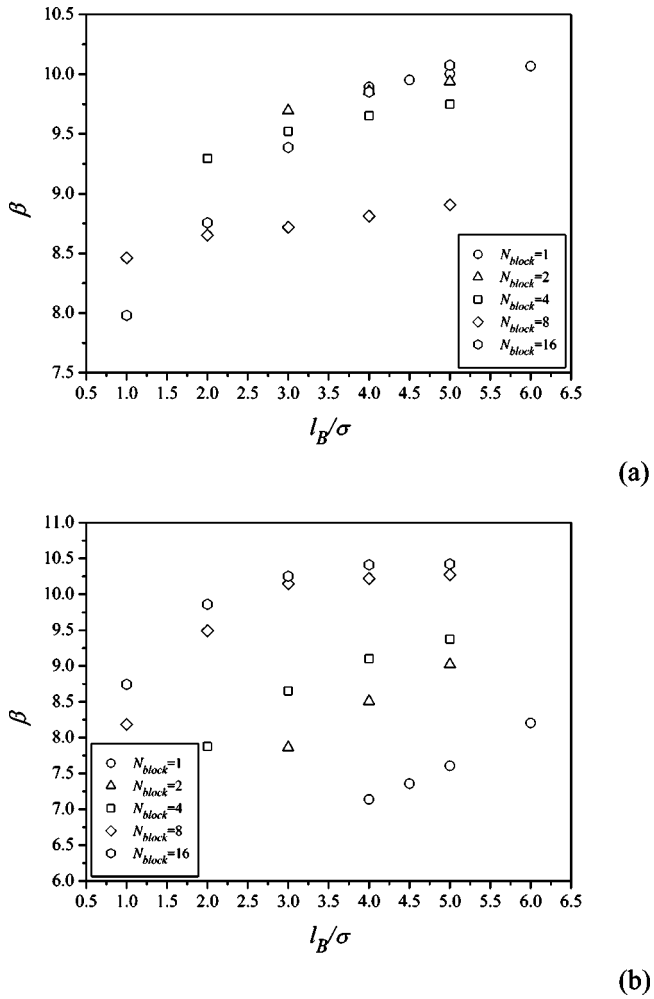

FIG. 13. The shape ratio β of (a) a polyelectrolyte and (b) a block polyampholyte as a function of the Bjerrum length l_B.

at the value of the Bjerrum length $l_B=3\sigma$. Thus a polyampholyte with $N_{block}=8$ and 16 at the value of the Bjerrum length $l_B=3\sigma$ approaches its fully extended conformation.

In Fig. 14, the largest value of the electric dipole moment

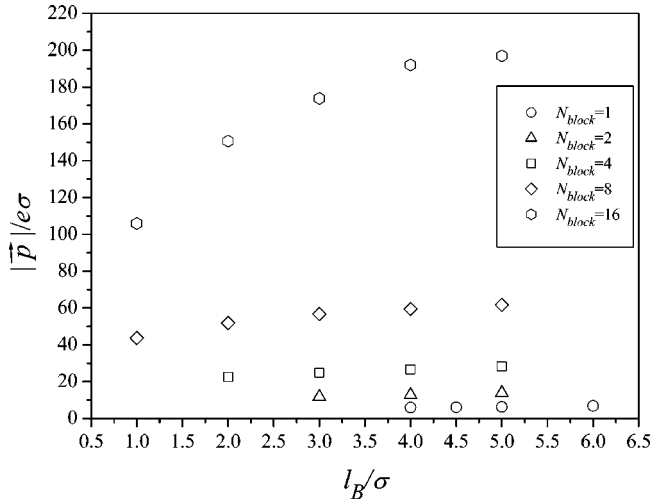

FIG. 14. Dependence of the absolute value of the dipole moment of the block polyampholyte on the Bjerrum length l_B.

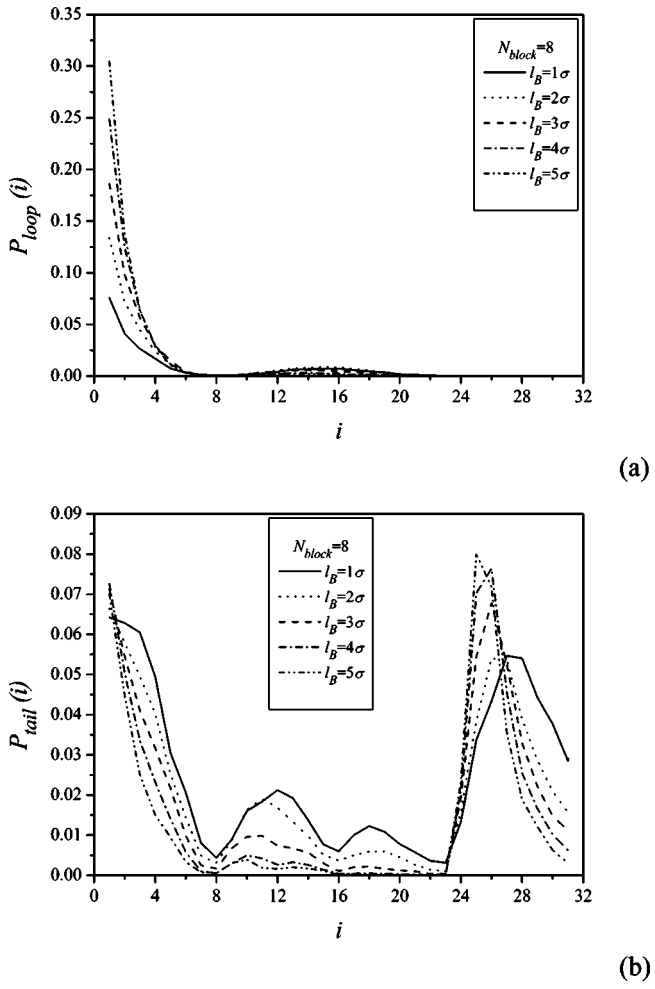

FIG. 15. (a) Loop $P_{loop}(i)$ and (b) tail $P_{tail}(i)$ distribution functions for block polyampholytes with $N_{block}=8$ at different values of the Bjerrum length.

$|\vec{p}|$ corresponds to a block polyampholyte with the longest block length. It is another indication of the fact that the block polyampholyte with longer periods of charge sequence are more easily polarizable and reach saturation faster. This saturation is in agreement with the leveling off behavior seen in Fig. 13(b) for the shape ratio β of polyampholytes with $N_{block}=8$ and 16.

Figure 15 shows the dependence of tail and loop distribution functions (P_{tail} and P_{loop}) for the block polyampholytes with $N_{block}=8$ on the different values of the Bjerrum length. Such a polyampholyte has two positively and two negatively charged blocks. There are two possible complex structures: either one positive charged block or both positive charged blocks are in contact with a negatively charged polyelectrolyte. If both positively charged blocks are in contact with a polyelectrolyte, the loop distribution function $P_{loop}(i)$ should be nonzero in the interval $8<i<24$. Figure 15(a) shows the opposite: the probability to find a loop in the interval $8<i<24$ is almost zero while the function $P_{loop}(i)$ is large in the interval $1\leqslant i\leqslant 8$, thus supporting the fact that only the end block is in contact with a polyelectrolyte. This is further collaborated by the shape of the tail distribution function $P_{tail}(i)$ shown in Fig. 15(b). The tail distribution function is nonzero in the intervals $i<8$ and $i>23$. The shapes of tail and loop distribution functions for block polyampholytes with $N_{block}=1$, 2, and 4 are similar to those shown in Fig. 9 for alternating polyampholytes which can be considered as block polyampholytes with period one. The only difference is the period of the zig-zag [see Figs. 2(b), 12(a), and 12(b)].

E. Model of polyampholyte-polyelectrolyte complexes

In this section, we will discuss a theoretical model of polyampholyte-polyelectrolyte complexes. Consider random symmetric polyampholyte chains of degree of polymerization N with equal fractions of positively $f_+=f/2$ and negatively $f_-=f/2$ charged monomers in a θ-solvent for the polymer backbone. Such a chain will keep its Gaussian shape if the intrachain electrostatic interactions are weaker than the thermal energy k_BT. The intrachain electrostatic interactions can be estimated as the energy of electrostatic interactions between two halves of a chain separated by a typical distance $R_0\approx bN^{1/2}$, where b is the bond length. For random polyampholytes, a typical charge imbalance in two halves of the chain is proportional to $e\sqrt{fN}$. Thus the intrachain electrostatic interactions are of the order of k_BTl_BfN/R_0. These interactions are weak and chain conformations remain almost unperturbed by these interactions if the fraction of charged groups f is smaller than $f_{weak}\approx 1/u\sqrt{N}$, where parameter u is the ratio of the Bjerrum length l_B to the bond length b. In our simulations, polyampholytes are strongly charged and the parameter f is equal to unity. Such strongly charged polyampholytes form a globule [24,48]. The equilibrium density ρ inside the polyampholyte globule is determined by balancing the fluctuation-induced attractive interactions $-k_BTR^3/r_D^3$ with the three-body repulsion $k_BTN(\rho b^3)^2$, where $r_D\approx(l_BNf/R^3)^{-1/2}$ is the Debye radius within a globule and R is the size of the globule. This results in the monomer density $\rho\approx ufb^{-3}$ and globular size $R\approx(N/\rho)^{1/3}\approx bN^{1/3}(uf)^{-1/3}$. The bulk free energy [48,49] of a polyampholyte globule is

$$F_{bulk}\propto -k_BTNu^2f^2. \tag{11}$$

The polyampholyte globule can be viewed as a droplet of concentrated polyampholyte solution of Gaussian strands with size R and the number of monomers in each strand being $g\approx R^2/b^2\approx(N/uf)^{2/3}$.

To begin with, let us consider complexation of a random polyampholyte with a rodlike infinitely long polyelectrolyte chain with linear charge density $e\rho_{PE}$. This approximation of an infinitely long polyelectrolyte chain is correct as long as the polyampholyte is located close to the middle of a polyelectrolyte chain of a finite length at distances r smaller than the length L_{PE} of a polyelectrolyte chain. An electric field created by the uniformly charged polyelectrolyte chain with a linear number charge density $\rho_{PE}=N/L_{PE}$ at distance r is

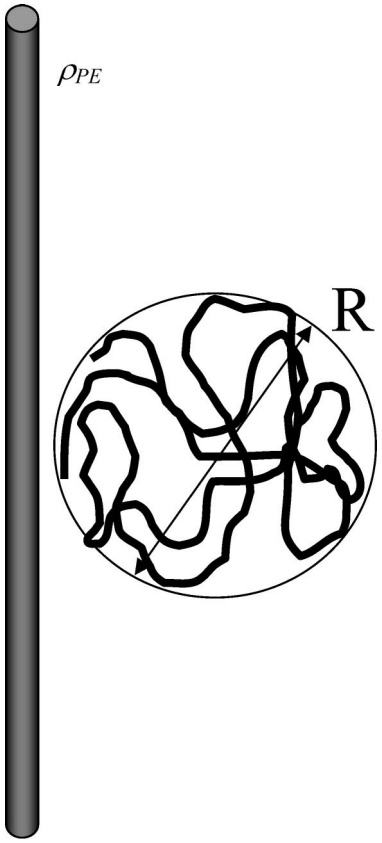

FIG. 16. Schematic sketch of polyampholyte globule near a rodlike polyelectrolyte.

$$E(r)=\frac{e\rho_{PE}}{2\pi\varepsilon r} \quad \text{for} \quad r\gg L_{PE}. \tag{12}$$

When placed near a polyelectrolyte chain, the polyampholyte globule is polarized by orienting its strands with g monomers along the electric field (see Fig. 16). Each strand of g monomers typically has a charge imbalance in two halves of a strand of the order of $e\sqrt{fg}$. The orientational polarizability α of the dipole with the dipole moment $p(g) \propto eR\sqrt{fg}$ can be estimated as e^2R^2fg/k_BT. The polarization energy of each strand in the external electric field $E(R)$ is

$$W_{pol}(g)\approx -\alpha E(R)^2\approx -k_BTl_B^2\rho_{PE}^2fg. \tag{13}$$

Thus, the total polarization energy of a random polyampholyte chain is equal to the number of strands per chain, N/g, times the polarization energy of a strand $W_{pol}(g)$,

$$W_{pol}\approx\frac{N}{g}W_{pol}(g)\approx -k_BTl_B^2\rho_{PE}^2fN. \tag{14}$$

The polarization energy of a randomly charged polyampholyte chain is proportional to the total number of charges on a chain fN. This polarization energy is proportional to the square of the so-called Oosawa-Manning condensation parameter $l_B\rho_{PE}$.

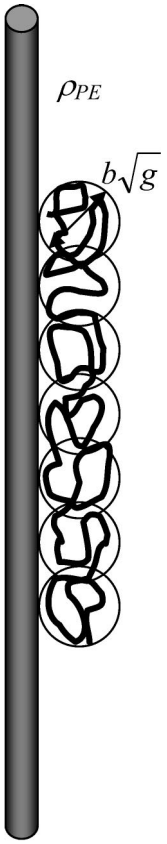

FIG. 17. Schematic sketch of polyampholyte-polyelectrolyte complex above the transition threshold.

It is easy to show that the polyampholyte globule is stable with respect to gradual deformations from increasing the linear charge density on the polyelectrolyte backbone. To see this, it is sufficient to estimate the energy of the cylindrical globule of length L_{PA} and thickness ξ. For such a globule the leading term in the polarization energy is similar to that for a spherical globule and is given by Eq. (14). But the surface energy of cylindrical globule will be higher than that of a spherical one, thus precluding globule elongation.

To complete the analysis of the globule stability, it is necessary to consider its global stability by comparing the energy of a polarized polyampholyte globule with that of a completely dissolved polyampholyte globule whose structure is exclusively controlled by an external electric field. In this case, the polyampholyte chain in the complex is divided into blobs with a Gaussian chain conformation within each blob (see Fig. 17). This structure will be locally stable if the intrablob electrostatic interactions are weaker than the thermal energy k_BT. This is true if the number of monomers in a blob g is smaller than $(uf)^{-2}$ (One can arrive at this estimate by repeating the analysis presented in the beginning of this section for the collapse threshold of a polyampholyte chain for a chain section containing g monomers.) Each blob has polar-

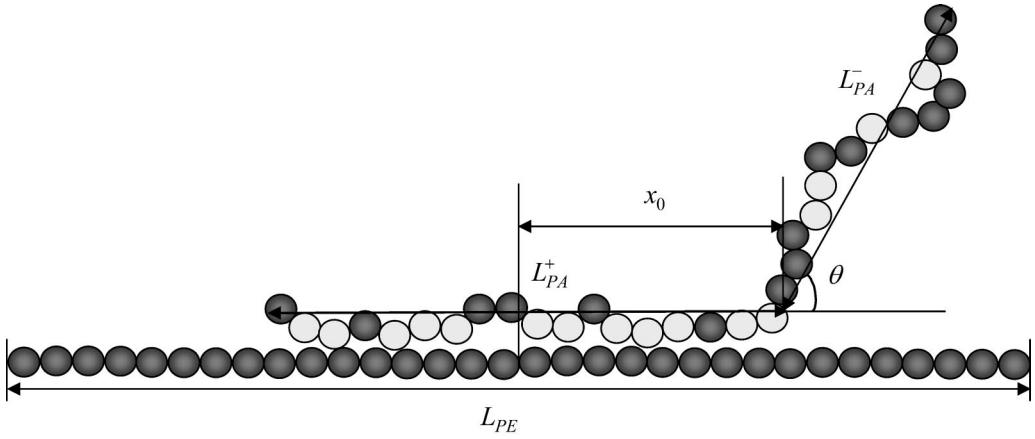

FIG. 18. Schematic sketch of a complex structure. Dark spheres represent negatively charged beads and white ones positively charged beads.

ization energy $W_{pol}(g) \approx -k_B T l_B^2 \rho_{PE}^2 f g$ of the order of the thermal energy $k_B T$. This leads to the number of monomers g in a blob to be equal to $g \approx (l_B^2 \rho_{PE}^2 f)^{-1}$. Thus, as the linear charge density on a polyelectrolyte chain increases, the number of monomers in a blob g decreases. The total polarization energy of a polyampholyte chain in this conformation is equal to the number of blobs on a chain N/g times the thermal energy $k_B T$, which leads us to the expression for polarization energy of a polyampholyte chain similar to Eq. (14) obtained for the polarization energy of a globule.

The polarized globule becomes globally unstable when its total free energy that includes both the bulk free energy of a globule Eq. (11) and polarization energy of a globule Eq. (14) becomes of the order of the polarization energy of the polarized Gaussian polyampholyte chain given by Eq. (14). This leads to the following estimate of the threshold value of the linear charge density of the polyelectrolyte chain,

$$\rho_{PE} \propto \sqrt{f}/b. \tag{15}$$

At this value of the linear charge density there exists the first-order transition between the polarized globule and the polarized Gaussian polyampholyte chain. For a fully charged random polyampholyte chain with $f=1$, this transition occurs when the distance between charged monomers on the polyelectrolyte chain is of the order of the bond length b.

The instability of a polyampholyte globule in a polyampholyte-polyelectrolyte complex can be seen in Fig. 1. At the initial stages of the simulation, the polyampholyte chain spreads itself over the polyelectrolyte and then moves towards the end of the polyelectrolyte chain. Above the instability threshold ($\rho_{PE} > \sqrt{f}/b$), the external electric field created by polyelectrolyte macromolecules controls the conformation of the polyampholyte in a complex. In this case the intrachain electrostatic interactions between charged monomers on the polyampholyte can be neglected and in developing the theoretical model of a complex we can only take into account interchain electrostatic interactions.

In our theoretical model of a polyampholyte-polyelectrolyte complex, a polyelectrolyte chain is assumed to be in a strongly elongated configuration and is represented by a rodlike chain of length L_{PE} (see Fig. 18). A randomly charged polyampholyte chain is modeled by a charged diblock polyampholyte. These blocks carry charges $\pm e\sqrt{N_{PA} f}$ and are having lengths L_{PA}^{+} and L_{PA}^{-} for positively and negatively charged blocks, respectively. The relative orientation of two blocks with respect to each other is controlled by the angle θ. (See Fig. 18 for a definition of length scales.) In our model we will assume that the oppositely charged block is aligned parallel to the polyelectrolyte backbone at a distance d from its axis. The junction point between two blocks is located at distance x_0 from the center of mass of the polyelectrolyte chain. The free energy of a polyampholyte chain in a complex $F_{complex}$ has two contributions. The first contribution is associated with the electrostatic energy U_{elect} of a polyampholyte chain in a complex

$$\frac{U_{elect}}{k_B T} = -\frac{l_B N_{PE} N_{PA}^{1/2}}{L_{PE} L_{PA}^{+}} \int_{-L_{PE}/2}^{L_{PE}/2} \int_0^{L_{PA}^{+}} \frac{ds\, ds'}{\sqrt{d^2 + (x_0 - s - s')^2}} + \frac{l_B N_{PE} N_{PA}^{1/2}}{L_{PE} L_{PA}^{-}} \int_{-L_{PE}/2}^{L_{PE}/2} \int_0^{L_{PA}^{-}} \frac{ds\, ds'}{\sqrt{(d + s\sin\theta)^2 + (x_0 + s\cos\theta - s')^2}}$$

$$+ \frac{l_B N_{PA}}{2 L_{PA}^{+2}} \int_0^{L_{PA}^{+}} \int_0^{L_{PA}^{+}} \frac{ds\, ds'}{\sqrt{(s-s')^2}} + \frac{l_B N_{PA}}{2 L_{PA}^{-2}} \int_0^{L_{PA}^{-}} \int_0^{L_{PA}^{-}} \frac{ds\, ds'}{\sqrt{(s-s')^2}} - \frac{l_B N_{PA}}{L_{PA}^{+} L_{PA}^{-}} \int_0^{L_{PA}^{+}} \int_0^{L_{PA}^{-}} \frac{ds\, ds'}{\sqrt{s^2 + s'^2 + 2ss'\cos\theta}}, \tag{16}$$

where the first and the second terms on the right-hand side of Eq. (16) describe the electrostatic interactions between the polyampholyte and the polyelectrolyte and the last three terms are the electrostatic self-energy of the block polyampholyte. The second contribution to the free energy is due to the polyampholyte chain elasticity. This elastic energy F_{elast} can be written as a sum of the elastic of two blocks,

$$\frac{F_{elast}}{k_BT}=\frac{N_{PA}}{2}\left[\beta_+\coth(\beta_+)-\ln\left(\frac{\sinh(\beta_+)}{\beta_+}\right)+\beta_-\coth(\beta_-)\right.$$
$$\left.-\ln\left(\frac{\sinh(\beta_-)}{\beta_-}\right)-2\right], \tag{17}$$

where $\beta_\pm$ is related to the block length of the polyampholyte through the following equation:

$$L_{PA}^{\pm}=\frac{N_{PA}b}{2}[\coth(\beta_\pm)-1/\beta_\pm]. \tag{18}$$

The equilibrium structure of a polyampholyte chain in a complex as a function of the Bjerrum length l_B and the position of the junction point x_0 is obtained by minimizing the chain free energy with respect to block lengths L_{PA}^+ and L_{PA}^-, angle θ, and distance d. During minimization, the distance d between two chains always decreases to the monomer size σ, due to the fact that it was kept constant at σ.

Figure 19(a) shows how the free energy of a complex $F_{complex}$ depends on the position of the junction point at the different values of the Bjerrum length. This plot shows that the free energy of the complex gradually decreases towards the chain end and then starts to increase as it goes beyond the end of the polyelectrolyte chain. The probability of finding a particular complex conformation is proportional to $\exp(-F_{complex}/k_BT)$. This probability distribution function is plotted in Fig. 19(b). Here it is shown that the complex forms with the highest probability at the end of the polyelectrolyte chain. The amplitude of the distribution function maximum increases with the Bjerrum length l_B. The distribution is similar to that shown in Fig. 3(a) except for a small shift in the peak position due to contraction of the polyelectrolyte chain that was ignored in our complex model.

Block lengths L_{PA}^+ and L_{PA}^-, angle θ, and the free energy of a complex $F_{complex}$ at the Bjerrum length $l_B=5\sigma$ are tabulated in Table I. The length of the positively charged block L_{PA}^+ increases from 5.9σ to 12.2σ while the negatively charged block L_{PA}^- decreases from 11.1σ to 9.0σ as the polyampholyte chain moves towards the end of the polyelectrolyte chain. The angle θ formed by two blocks of the polyampholyte is equal to 110° (the two blocks are almost perpendicular to each other) in the middle of the polyelectrolyte chain and 11° (the two blocks are almost perfectly aligned with each other) at the end of the polyelectrolyte chain. These results agree well with snapshots shown in Fig. 1; therefore, our theoretical model successfully explains the structure of random polyampholyte-polyelectrolyte complexes.

Since complexes between block polyampholytes with $N_{block}=8$ and 16 and polyelectrolyte chains have the double

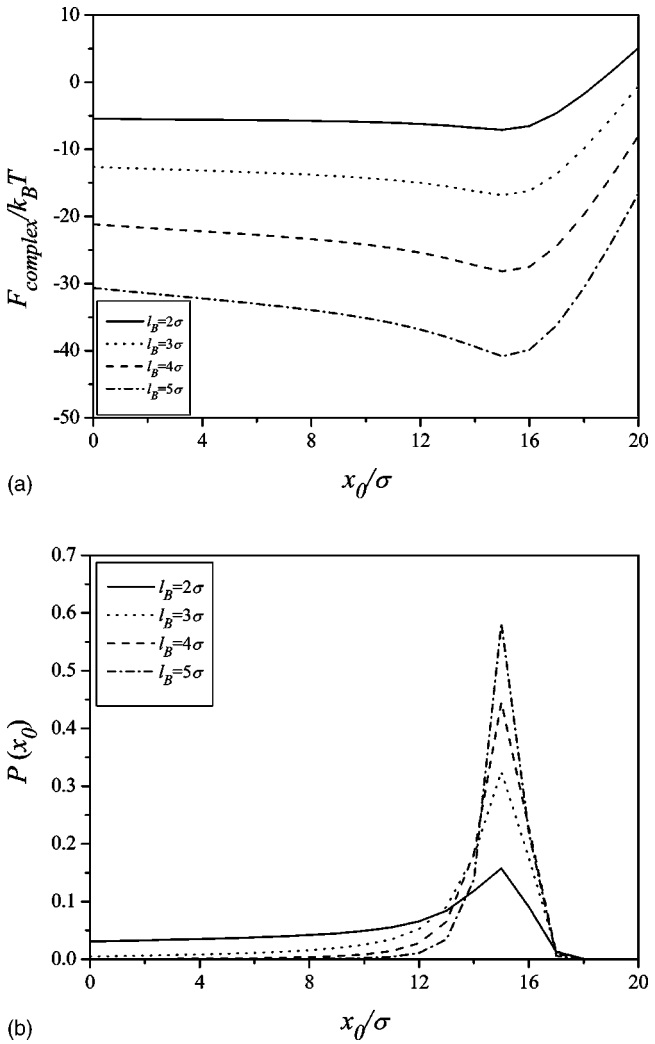

FIG. 19. Dependence of (a) the complex free energy $F_{complex}$ and (b) corresponding distribution function $P(x_0)$ on the position of the junction point x_0 for different values of the Bjerrum length.

helix structure, we modified the rail-track model [50–52] shown in Fig. 20 to calculate electrostatic energy U_{elect} of a double helix as a function of the twist angle ψ. Figure 21 shows the dependence of the repulsive and attractive parts of the electrostatic energy on the twist angle ψ at the value of the Bjerrum length $l_B=4\sigma$ as the complex transforms from two parallel chains to a double helix. The twist angle value of $\psi=180°$ means that the positively charged block of the polyampholyte is parallel to the polyelectrolyte chain. The smallest value of the twist angle ψ is equal to 70.5° and is controlled by the hard-core interactions between monomers. The electrostatic energy of a double helix has a minimum at the value of the twist angle $\psi=70.5°$. This means that the helical structure is a linked set of tetrahedrons. This tendency is independent of the value of the Bjerrum length l_B.

When our calculations are expanded to the whole complex, the twist angle ψ, tilt angle θ at a junction point between blocks, and rotational angle $\varphi$with respect to the end-to-end vector of the double helix were adjusted to minimize complex electrostatic energy. After optimization of these parameters, the angles ψ, θ, and φ are equal to 70.5°, 13.5°, 20.0°, and respectively, regardless of the value of the Bjer-

TABLE I. Dependence of the equilibrium block lengths L_{PA}^{+}, L_{PA}^{-}, angle θ, and free energy $F_{complex}$ of the complex on the position of the junction point x_0 at the Bjerrum length $l_B=5\sigma$.

x_0/σ	L_{PA}^{+}/σ	L_{PA}^{-}/σ	θ (deg)	$F_{complex}/k_BT$
0	5.9	11.1	110.5	−30.6
1	6.1	11.1	108.2	−31.1
2	6.2	11.1	106.0	−31.4
3	6.5	11.2	103.7	−31.8
4	6.6	11.2	101.5	−32.2
5	6.8	11.2	99.1	−32.6
6	7.0	11.2	96.5	−33.0
7	7.2	11.2	93.7	−33.5
8	7.4	11.2	90.5	−34.0
9	7.6	11.2	86.9	−34.5
10	7.9	11.1	82.5	−35.1
11	8.2	11.1	77.0	−35.9
12	8.5	11.1	70.1	−36.9
13	8.9	11.0	60.9	−38.0
14	9.3	10.8	48.5	−39.4
15	9.8	10.4	33.2	−40.8
16	10.4	10.0	21.3	−39.9
17	11.0	9.7	15.9	−36.2
18	11.5	9.4	13.2	−30.6
19	11.9	9.2	11.8	−23.9
20	12.3	9.0	11.1	−16.5

rum length l_B. Furthermore, about five monomers of a block polyampholyte form the unit pitch in a double helix structure. This explains why only block polyampholytes with $N_{block}=8$ and 16 form a double helix with a polyelectrolyte chain.

IV. CONCLUSIONS

We have analyzed the effect of a charge sequence on the complex formation between polyampholyte and polyelectrolyte chains. Our Monte Carlo simulations have confirmed the notion that the complexation between polyampholytes and polyelectrolytes is driven by polarization-induced attraction. Independent of charge sequence, the complex is preferentially formed at the end of a polyelectrolyte chain. This complex structure allows maximizing the electrostatic attraction between oppositely charged sections of the polyampholyte chain and polyelectrolyte backbone while at the same time minimizing the electrostatic repulsion between similarly charged sections of the polyampholyte and the polyelectrolyte. Block polyampholytes with long blocky charge sequences form a double helix with the polyelectrolyte backbone. This helical structure appears first for the block polyampholytes with $N_{block}=8$. For shorter blocky sequences, it is hard to establish the formation of a double helix because at least five monomers per strand are required to complete a pitch of the double helix. Thus, charged blocks with $N_{block}\leqslant 4$ are too short to form a well-defined double helix. The parameters of the double helix are not very sensitive to the strength of the electrostatic interactions. Instead of a double helix, oppositely charged monomers of a random polyampholyte form loops with the polyelectrolyte backbone. The number of bonds in a loop as well as its typical size decrease with increasing strength of the electrostatic interactions.

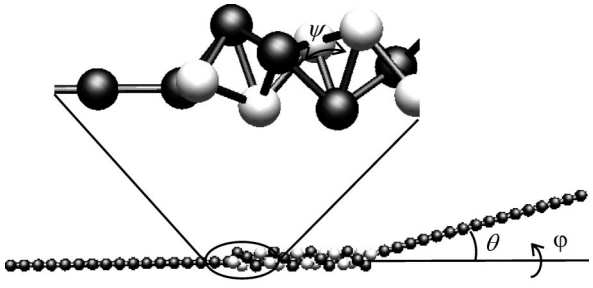

FIG. 20. Schematic sketch of a complex formed by block polyampholyte with $N_{block}=16$ and polyelectrolyte chain. The twist, tilt, and rotational angles are denoted by ψ, θ, and φ, respectively. Dark spheres represent negatively charged beads and white ones positively charged beads.

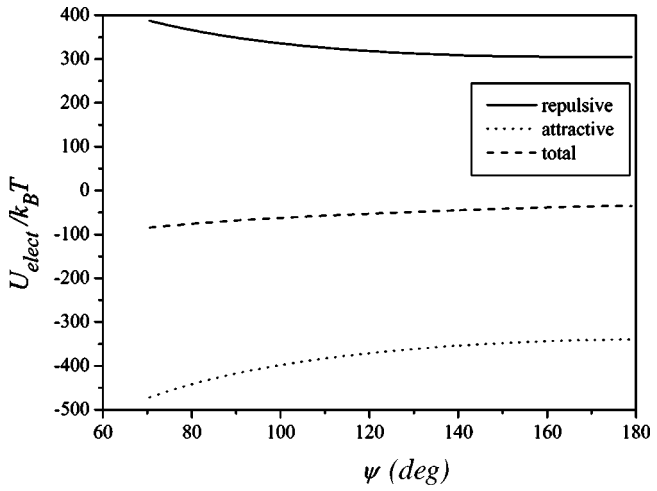

FIG. 21. Dependence of the electrostatic energy of double helix on the twist angle ψ for $l_B=4\sigma$. The solid, dotted, and dashed lines represent the repulsive, attractive, and total electrostatic energy, respectively.

Our simulations have also shown that collapsed polyampholytes undergo a coil-globule phase transition during complex formation. This can be seen in the snapshot sequence shown in Fig. 1 representing the evolution of the chain conformations during the simulation run.

We have neglected counterions in our simulations. It is believed that counterions can facilitate complexation between polyampholytes and polyelectrolytes. Often, the large contribution to the free energy of binding between polyampholytes and polyelectrolytes comes from the counterions released from the polyelectrolyte [53–56]. For example, a polyampholyte has many positively charged monomers that can bind to a negatively charged polyelectrolyte. These positively charged monomers partially stabilize the large negative charge that causes counterions to condense on the anionic polyelectrolyte in the absence of polyampholyte. This

stabilization allows a bound protein to release multiple counterions from the polyelectrolyte. Entropy thus contributes significantly to a large portion of the binding free energy. This effect of counterion release during complex formation is the subject of our current study. Our preliminary results thus far show that counterion release does not in fact change the final complex structure in dilute solutions. A polyampholyte preferentially binds to the end of the polyelectrolyte chain. The details of this study will be presented in future publications.

ACKNOWLEDGMENT

We are grateful to the University of Connecticut Research Foundation for the financial support.

[1] *Polyelectrolytes*, edited by M. Hara (Marcel Dekker, New York, 1993).
[2] C. Tanford, *Physical Chemistry of Macromolecules* (Wiley, New York, 1961).
[3] F. Oosawa, *Polyelectrolytes* (Marcel Dekker, New York, 1971).
[4] M. Mandel, in *Encyclopedia of Polymer Science and Engineering*, edited by H. F. Mark, N. M. Bikales, C. G. Overberger, and G. Mendes (Wiley, New York, 1988).
[5] K. S. Schmitz, *Macroions in Solution and Colloidal Suspension* (VCH, Weinheim, 1993).
[6] S. Forster and M. Schmidt, Adv. Polym. Sci. **120**, 51 (1995).
[7] J. L. Barrat and J. F. Joanny, Adv. Chem. Phys. **94**, 1 (1996).
[8] *Physical Chemistry of Polyelectrolytes*, edited by T. Radeva (Marcel Dekker, New York, 2001).
[9] *Colloid-Polymer Interactions: From Fundamentals to Practice*, edited by P. L. Dubin and R. S. Farinato (Wiley, New York, 1999).
[10] E. Kokufuta, Polym. Prepr. (Am. Chem. Soc. Div. Polym. Chem.) **32**, 604 (1991).
[11] J. Y. Shieh and C. E. Glatz, Polym. Prepr. (Am. Chem. Soc. Div. Polym. Chem.) **32**, 606 (1991).
[12] J. M. Park, B. B. Muhoberac, P. L. Dubin, and J. Xia, Macromolecules **25**, 290 (1992).
[13] J. Xia, P. L. Dubin, Y. Kim, and B. B. Muhoberac, J. Phys. Chem. **97**, 4528 (1993).
[14] L. S. Ahmed, J. Xia, P. L. Dubin, and E. Kokufuta, J. Macromol. Sci., Pure Appl. Chem. **31**, 17 (1994).
[15] *Macromolecular Complexes in Chemistry and Biology*, edited by P. Dubin, J. Bock, R. M. Davies, D. Schulz, and C. Thies (Springer-Verlag, Berlin, 1994).
[16] V. A. Izumrudov, Ber. Bunsenges. Phys. Chem. **100**, 1017 (1996).
[17] A. Tsuboi, T. Izumi, M. Hirata, J. Xia, P. L. Dubin, and E. Kokufuta, Langmuir **12**, 6295 (1996).
[18] W. A. Bowman, M. Rubinstein, and J. S. Tan, Macromolecules **30**, 3262 (1997).
[19] N. Pernodet, D. Gersappe, J. Sokolov, M. Rafailovich, and K. McLeod, Bull. Am. Phys. Soc. **45**, 519 (2000).
[20] D. A. Swann, J. B. Caulfield, and A. Ceselski, Ann. Rheum. Dis. Suppl. **34**, 98 (1975).
[21] D. A. Swann and J. B. Caulfield, Connect. Tissue Res. **4**, 31 (1975).
[22] D. A. Swann, in *The Joints and Synovial Fluid*, edited by L. Sokoloff (Academic, New York, 1978).
[23] W. E. Krause, Ph.D. thesis, Pennsylvania State University, 2000.
[24] A. V. Dobrynin, M. Rubinstein, and J. Joanny, Macromolecules **30**, 4332 (1997).
[25] R. R. Netz and J. Joanny, Macromolecules **31**, 5123 (1998).
[26] A. V. Dobrynin, S. P. Obukhov, and M. Rubinstein, Macromolecules **32**, 5689 (1999).
[27] E. B. Zhulina, A. V. Dobrynin, and M. Rubinstein, Eur. Phys. J. E **5**, 41 (2001).
[28] A. V. Dobrynin, E. B. Zhulina, and M. Rubinstein, Macromolecules **34**, 627 (2001).
[29] E. B. Zhulina, A. V. Dobrynin, and M. Rubinstein, J. Phys. Chem. B **105**, 8917 (2001).
[30] H. Schiessel, G. Oshanin, and A. Blumen, J. Chem. Phys. **103**, 5070 (1995).
[31] H. Schiessel, G. Oshanin, and A. Blumen, Macromol. Theory Simul. **5**, 45 (1996).
[32] H. Schiessel and A. Blumen, J. Chem. Phys. **104**, 6036 (1996).
[33] H. Schiessel and A. Blumen, J. Chem. Phys. **105**, 4250 (1996).
[34] R. G. Winkler and P. Reineker, J. Chem. Phys. **106**, 2841 (1997).
[35] H. G. Curme and C. C. Natale, J. Phys. Chem. **68**, 3009 (1964).
[36] R. Berendsen and H. Borginon, J. Photogr. Sci. **16**, 194 (1968).
[37] T. Maternaghan, O. B. Banghan, and R. H. Ottewill, J. Photogr. Sci. **28**, 1 (1980).
[38] *Proteins at Interfaces*, edited by A. T. Kudish and F. R. Eirich (American Chemical Society, Washington, DC, 1987).
[39] N. Kawanishi, H. K. Christenson, and B. W. Ninham, J. Phys. Chem. **94**, 4611 (1990).
[40] A. K. Vaynberg, N. J. Wagner, R. Sharma, and P. Martic, J. Colloid Interface Sci. **205**, 131 (1998).
[41] Y. Kamiyama and J. Israelachvili, Macromolecules **25**, 5081 (1992).
[42] S. Neyret, L. Ouali, F. Candau, and E. Pefferkorn, J. Colloid Interface Sci. **187**, 86 (1995).
[43] J. H. E. Hone, A. M. Howe, and T. H. Whitesides, Colloids Surf., A **161**, 283 (2000).
[44] G. Grest and M. Murat, Macromolecules **26**, 3108 (1993).
[45] M. Lal, Mol. Phys. **17**, 57 (1969).
[46] N. Madras and A. D. Sokal, J. Stat. Phys. **50**, 109 (1988).
[47] R. G. Winkler, M. O. Steinhauser, and P. Reineker, Phys. Rev. E **66**, 021802 (2002).
[48] P. G. Higgs and J. F. Joanny, J. Chem. Phys. **94**, 1543 (1991).
[49] A. V. Dobrynin and M. Rubinstein, J. Phys. II **5**, 677 (1995).
[50] R. Everaer, R. Bundschuh, and K. Kremer, Europhys. Lett. **29**, 263 (1995).
[51] T. B. Liverpool, R. Golestanian, and K. Kremer, Phys. Rev. Lett. **80**, 405 (1998).

[52] R. Golestanian and T. B. Liverpool, Phys. Rev. E **62**, 5488 (2000).
[53] M. T. Record, T. M. Lohman, and P. de Haseth, J. Mol. Biol. **107**, 145 (1976).
[54] M. T. Record, C. F. Anderson, and T. M. Lohman, Quart. Rev. Biophys. **11**, 103 (1978).
[55] D. P. Mascotti and T. M. Lohman, Proc. Natl. Acad. Sci. U.S.A. **87**, 3142 (1990).
[56] B. Jayaram, F. M. DiCapua, and D. L. Beveridge, J. Am. Chem. Soc. **113**, 5211 (1991).